Propulsion and Power Research 2015;4(2):63–71

HOSTED BY

ELSEVIER

http://ppr.buaa.edu.cn/

Propulsion and Power Research

www.sciencedirect.com

ORGINAL ARTICLE

Quick fabrication of aeronautical complicated structural parts based on stereolithography

Jiangping Zhou[a,b], Zhongliang Lu[a,b,*], Kai Miao[a,b], Zhe Ji[a,b], Yin Dong[c], Dichen Li[a]

[a]*State Key Laboratory for Manufacturing Systems Engineering, Xi'an Jiaotong University, Xi'an 710049, China*
[b]*Collaborative Innovation Center for Advanced Aero-Engine, Beijing 100191, China*
[c]*Xi'an Aerospace Power Investment Casting Company (GROUP) Ltd, Xi'an, China*

Received 29 October 2014; accepted 29 January 2015
Available online 17 June 2015

KEYWORDS

Stereolithography;
Surface roughness;
Thermal stress;
Turbine stator

Abstract Investment casting based on stereolithography (SL) has the characteristics of short production cycle and low cost, which is especially suitable for fabricating complex aeronautical parts without metal dies. But there are some problems during the fabrication process, such as low surface accuracy caused by the staircases of resin prototype, shell cracking caused by higher thermal stress during the sintering process and so on. Taking an engine turbine stator as a fabrication example, the surface accuracy of resin prototype under the effect of coating method was investigated using the laser confocal microscopy; what's more, both theoretical analysis and finite element analysis (FEA) were combined and compared to reveal the thermal stress field of ceramic shell during pyrolyzing and sintering process under different situation. It was founded that the surface staircases of the resin prototype was eliminated and the surface quality was improved after coating process, the thermal stress was decreased and shell cracking was avoided by sintering the ceramic shell with the inner hollow resin prototype under the heating rate of 5 °C/min. The result showed that, the metal turbine stator had high dimensional accuracy of CT4-CT6 and had a good surface finish within R_a 3.2.

1. Introduction

Engine turbine stator is the key part of aero-engine and gas turbine, which is generally fabricated through investment casting, and the metal dies are an essential tool to

*Corresponding author. Tel.: +86 29 82665126.
E-mail address: zllu@mail.xjtu.edu.cn (Zhongliang Lu).
Peer review under responsibility of National Laboratory for Aeronautics and Astronautics, China.

http://dx.doi.org/10.1016/j.jppr.2015.05.001

Nomenclature

H	layer's thickness (unit: mm)
L_w	width of laser beam (unit: mm)
C_d	resin's curing depth (unit: mm)
R_a	arithmetical mean deviation of profile (unit: mm)
T	thermodynamic temperature (unit: K)
b	radius of resin prototype (unit: mm)
a	radius of ceramic shell (unit: mm)
t	wall thickness of ceramic shell (unit: mm)

Greek letters

α	angle between upper surface of part and level (unit: rad)
θ	angle between actual profile line and normal line of upper surface (unit: rad)
γ	staircase's height which is the distance between actual contour line's nadir and theory contour line (unit:mm)
δ	stress (unit: MPa)
τ	coefficient of thermal expansion (unit: W/(m$^2 \cdot$ K))
σ	bending strength (unit: MPa)
v	Poisson ratio
G	shear modulus (unit: Pa)

Subscripts

δ_r	radial stress (unit: MPa)
δ_β	hoop stress (unit: MPa)
σ_{slim}	bending strength of ceramic shell (unit: MPa)
τ_1	coefficient of thermal expansion of ceramic (unit:W/(m$^2 \cdot$ K))
τ_2	coefficient of thermal expansion of resin (unit: W/(m$^2 \cdot$ K))
G_1	shear modulus of ceramic (unit: Pa)
G_2	shear modulus of resin (unit: Pa)

make wax pattern for investment casting. With the improvement of engine comprehensive performance, the structure of turbine stator is becoming more complex, and the corresponding structure of metal dies also has to be changed. Resulting in many problems during fabrication process of complex part based on investment casting, such as long production cycle, high cost and low yield. Therefore it cannot quickly meet the market's needs for new complex metal parts in single and small batch production [1].

Stereolithography (SL) is a new technology based on layered manufacturing which is the most common among all the RP techniques. Owing to the SL's characteristic of layer forming mechanism, complex parts can be fabricated directly in a short time without metal dies which can be used to replace wax pattern in investment casting. Therefore the quick casting (QC), which combines stereolithography and investment casting, has many advantages in producing complex parts in single and small batch production, such as short production cycle, low cost and simple process, which is especially suitable for fabricating complex metal parts in small series production [1,2]. During the QC process, the wax patterns are replaced by resin prototypes and complex metal parts are obtained after coating resin prototypes with

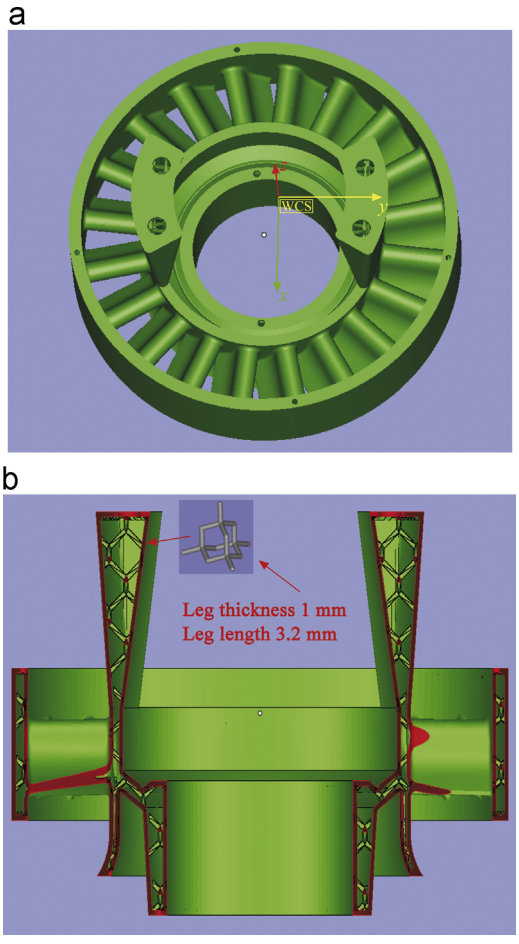

Figure 1 CAD model of turbine stator. (a) CAD model and (b) internal web structure.

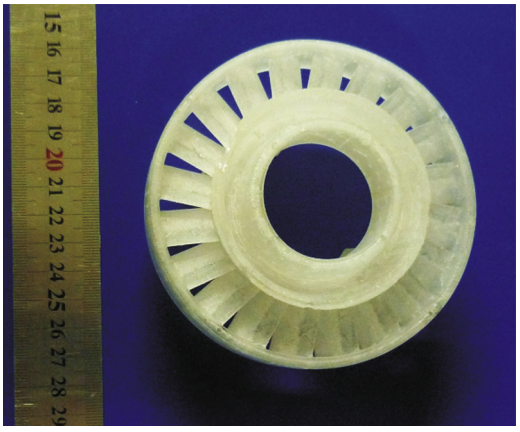

Figure 2 Resin prototype of turbine stator.

ceramic slurry, drying and hardening, pyrolyzing and sintering, metal casting.

However, there are also some problems during the fabrication process, such as the low surface accuracy of resin prototype caused by the layer forming mechanism of SL [3,4], which will result in low surface accuracy of metal parts after QC process for the reason that staircases of resin prototype' surface will be transferred to metal part's surface. What's more, ceramic shell may crack as high thermal stress caused by expansion of resin during the early stage of pyrolyzing and sintering process [5].

Combing with the fabrication example of engine turbine stator, the surface accuracy of resin prototype under effect of coating method was investigated using the laser confocal microscopy and surface roughness measuring instrument. In addition, the law of ceramic shell's thermal stress field was investigated by using thermal-structure indirect coupling function of ANSYS software; the bending strength of ceramic shell was tested using universal material machine, which can provide a reference for sintering process.

2. Experimental procedure

2.1. Fabrication

2.1.1. Design and fabrication of resin prototype

The CAD model for turbine stator was designed in UG (Unigraphics NX) and the model was converted into STL data, then the internal web structure of CAD model was designed in the Magics, finally the STL data was sliced into 0.1 mm layer thickness in Magics (Figure 1). The resin prototype of turbine stator was automatically fabricated based on the STL data by SL apparatus SPS 450B-(Institute of Advanced Manufacturing Technology in Xi'an Jiaotong University of China) (Figure 2).

2.1.2. Coating process

The resin prototype of turbine stator was coated with phenolic resin (PR) (Table 1). First the resin prototype was entirely dipped into the PR for several minutes, then resin prototype was taken out of liquid resin, and the micro trough of the surface was filled with PR due to the gravity and viscosity of liquid resin. After cleaning off the excess coating resin on surface, the coated resin prototype was moved into drying oven under temperature 40 °C, the PR can be cured on the resin prototype's surface after staying in the dry oven for 30-40 min [6]. Through post-processing, the surface roughness R_a is reduced from 4–20 μm to 3.2 μm.

2.1.3. Fabrication of green ceramic shell

After silicasol, zicon powder and defoamer were mixed together in the light of a certain proportion and were stirred for 24 h. The ceramic slurry of shell's face layer was acquired, and then the ceramic slurry of shell's back layer could be obtained in the same way using silicasol and Shangdian soil. The assembly of resin prototype and wax riser was repeatedly dipped and stuccoed with composite coating slurry, and then the green ceramic shell was achieved with wall thickness of 6-8 mm. After the green ceramic shell was dried for 48 h in the environment with temperature of 24-25 °C and humidity of 50%-60%, the intact green ceramic shell with resin prototype was gained (Figure 3).

2.1.4. Pyrolyzing and sintering process

After the green ceramic shell was completely dried, it was sintered in a furnace, making its inside resin prototype burned out completely, then the inner hollow ceramic shell was achieved.

2.1.5. Metal casting process

The molten steel was poured into the inner hollow ceramic shell under high environment temperature, and then metal turbine stator was obtained after cooling to room temperature.

2.2. Characterizations of specimens

The resin specimens were fabricated using 8981 resin, laser confocal microscopy (OLS4000, Japan) was used to measure the surface roughness and surface microstructure before and after coating process. And the coefficient of

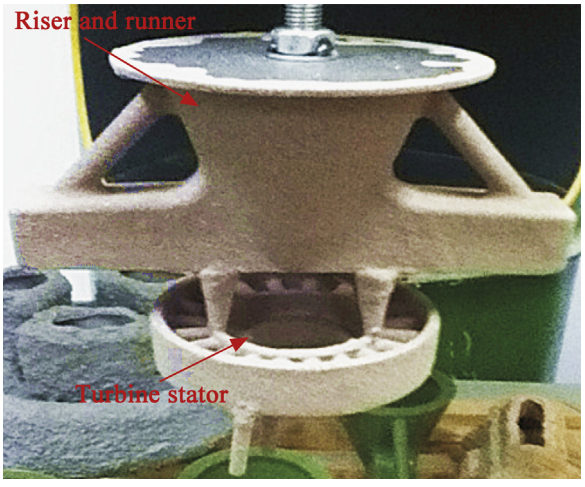

Figure 3 Green ceramic shell.

Table 1 Formula of PR coating.

Chemical constituent	PR	EG	Benzenesulonyl chloride	DMP
Mass fraction/(wt%)	62.11	31.05	0.062	0.006

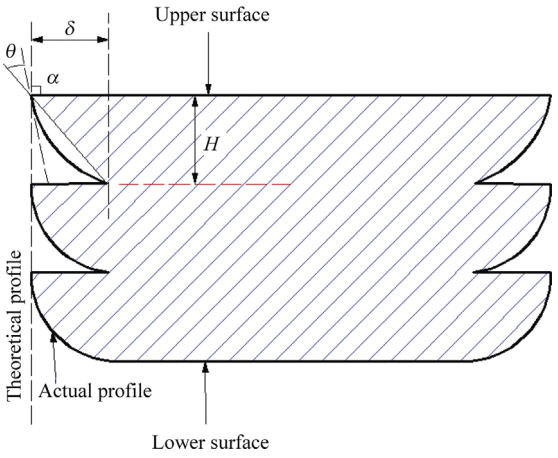

Figure 4 Model of staircases.

thermal expansion (CTE) of resin prototype was measured by thermal dilatometer (RPZ-16-10P, China)

The ceramic specimens (6 mm × 10 mm × 50 mm) was prepared on the basis of the above mentioned fabrication process of ceramic shell, and the three point bending strength of it was measured after heated from room temperature to 600 °C using universal material testing machine (HSST-6003QP, China).

Scanning electron microscopy (Hitachi S-3000N, Japan) was used to observe the microstructure of the ceramic specimens before and after sintering process.

3. Results and discussions

3.1. Surface roughness of resin prototype

3.1.1. Analysis of staircases

SL is an automatic construction method of physical objects using additive manufacturing technology, owing to the fabrication theory of SL that resin can be cured by exposure of laser beam, part's layer is fabricated orderly and heaped up together, then the three-dimensional part is got. As a result of SL's fabrication mechanism, there are unavoidable staircases on the surface of resin prototype.

According to manufacturing theory of SL, the analysis model of staircases was built (Figure 4). Where H is the layer's thickness, α is the angle between upper surface of part and level, θ is the angle between actual profile line and normal line of upper surface, which can be represented as Eq. (1) [7]

$$\theta = \tan^{-1}\left[\frac{L_w}{2H}\left(1-\sqrt{1-\frac{H}{C_d}}\right)\right] \tag{1}$$

Where L_w is the width of laser beam, C_d is resin's curing depth, γ is the staircase's height which is the distance between actual contour line's nadir and theory contour line. And the γ can be represented as Eq. (2):

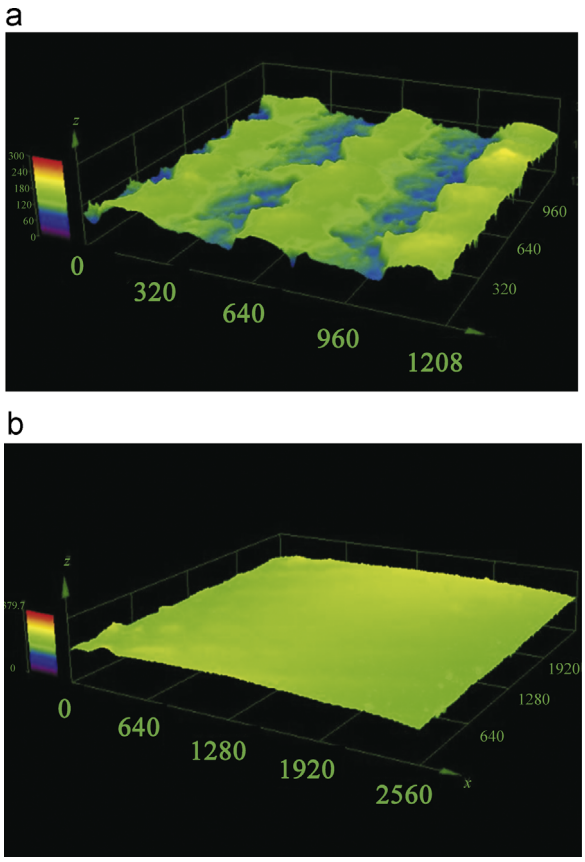

Figure 5 Microstructure of surface. (a) Uncoated surface and (b) coated surface.

$$\gamma = \frac{H}{\cos\theta}\cos(\alpha-\theta) \quad (\theta \neq 0) \tag{2}$$

R_a is arithmetical mean deviation of profile, which can be a parameter of surface finish. It can be represented as Eq. (3):

$$R_a = \frac{\frac{1}{4}\times\left[\gamma\times\frac{H}{\sin\alpha}+\varepsilon\times\sqrt{\left(\frac{H}{\sin\alpha}-c\tan\alpha\right)^2+\gamma^2}\right]}{\frac{H}{\sin\alpha}} \tag{3}$$

As the coefficient $\varepsilon\to 0$, then $R_a=\frac{1}{4}\gamma\delta$. So the R_a can be represented as Eq. (4):

$$R_a = \frac{1}{6}\frac{H}{\cos\theta}\cos(\alpha-\theta) \quad (\theta \neq 0) \tag{4}$$

3.1.2. Coating process

As the analysis of staircases above, there are unavoidable low surface roughness of R_a 4–20 μm. Therefore, if the staircases are not removed before the resin prototypes used as the wax pattern for investment casting, the staircases will be transferred to the surface of final metal product, resulting in metal product's low surface finish.

So the surface of resin prototype had to be post-processed. After coating process, the phenolic resin coating can be cured on the surface of resin prototype and staircases were eliminated, which will lead to a good surface finish.

Microstructure comparison between the surface of coated resin prototype and that of uncoated resin prototype is showed in Figure 5, before coating process, there are obvious staircases on the uncoated surface and the value of R_a is about 7.5 μm, after coating process, the valley of the staircases is filled with cured PR resin and the value of R_a decreases to about 1 μm.

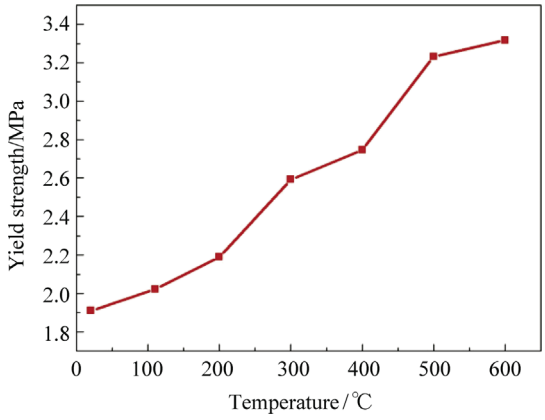

Figure 6 Bending strength of ceramic.

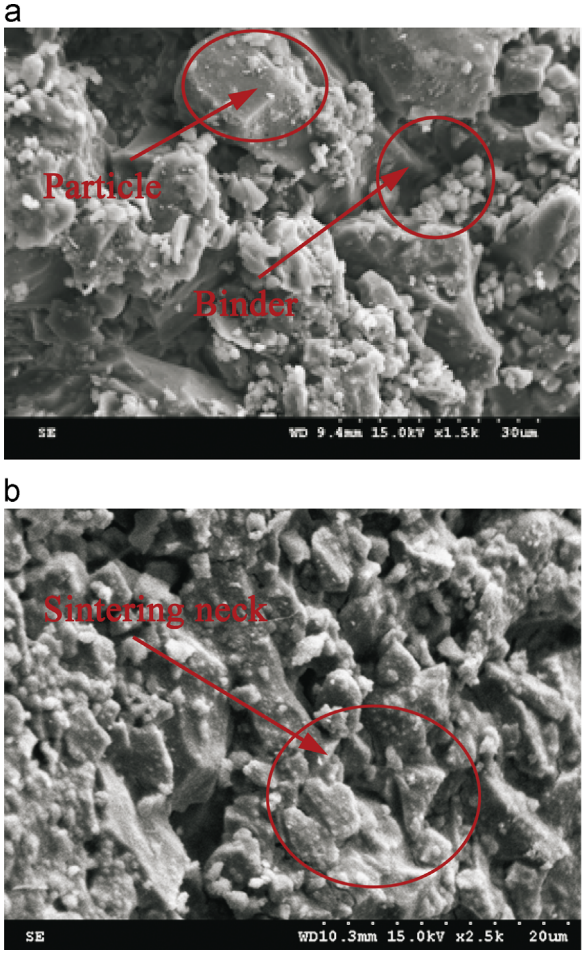

Figure 7 SEM of ceramic shell. (a) Back layer before sintering and (b) back layer after sintering.

3.2. *Analysis of pyrolyzing and sintering process*

3.2.1. *Bending strength under different temperature*

The ceramic specimens were heated from 20 °C to 600 °C, its bending strengths under different temperature are shown in Figure 6. The bending strength of ceramic is improved from 1.92 MPa to 3.318 MPa along with the temperature rising. The microstructures of the specimens before and after sintering are shown in Figure 7. After sintering process, the binder is burned out and the particles are densely sintered together which form the skeleton of ceramic shell, making the shell has high bending strength.

3.2.2. *Thermal expansion coefficient and burning performance*

The CTE of resin specimens was tested in the thermaldilatometer and was heated to 300 °C with different heating rates from 3 °C/min to 5 °C/min. During the temperature-rise period, the CTE were recorded automatically. Curves of CTE are shown in Figure 8. During the heating period, the three CTE curves increases dramatically from 20 °C to 300 °C, while the CTE curves drops significantly after 300 °C as

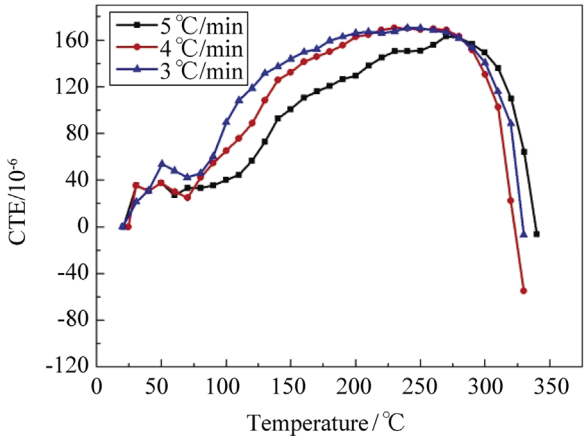

Figure 8 CTE of resin.

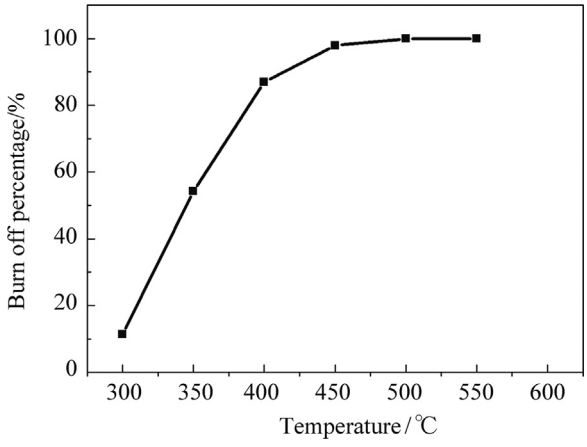

Figure 9 Burning off percentage of resin.

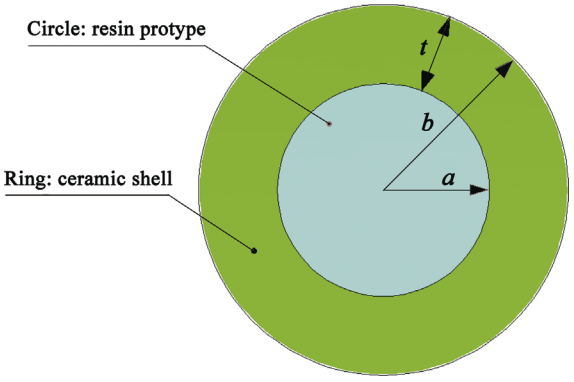

Figure 10 Theoretical cylindrical model.

resin is burned out largely. It also can be seen that, with the increment of heating rate, the CTE of resin decrease, and the CTE of resin under heating rate of 5 °C/min is lower than that under other heating rate before 300 °C.

The burning off percentage of resin under different temperature is tested and the curves of burning off percentage are shown in Figure 9. At heating temperature of 300 °C, 11.396 wt% of resin is burning out. After 300 °C, the burn off percentage of resin is rising with the increase of heating temperature, when the resin is heating to 400 °C, almost 98 wt% of resin is burning out, then with the temperature continue increase to 450 °C, the burn off percentage increase to 99.9 wt%, and after that, the weight of resin would not loss any more, that means the weight of resin ash after completely burning out is 0.1 wt% of unburned resin, so the ash is so little to blow away from the inner hollow ceramic shell by airbrush.

3.2.3. *Analysis of thermal stress*

A theoretical cylindrical model consisted of internal resin prototype and external ceramic shell is built (Figure 10). The analysis model is heated from T_0 to T_e with heating rate of 300 °C/h. Therefore the thermal stress of cylindrical model can be achieved by using displacement method [8].

The radial stress caused by squeezing action between resin prototype and ceramic shell is represented as Eq. (5).

$$\delta_r = \frac{[(1+v_2)\alpha_2 - (1+v_1)\alpha_1]T(b,t)}{\frac{1}{2G_1} + \frac{(1-v_1)a^2}{G_1(t^2+2at)} - \frac{1-2v_2}{2G_2}} \tag{5}$$

Supposing there is no difference between cylinder model's internal temperature and external temperature, and $b=a+t$, b is radius of resin prototype and a is radius of ceramic shell, t is the wall thickness of ceramic shell. So the hoop stress can be represented as Eq. (6):

$$\delta_\beta = \frac{[(1+v_2)\tau_2 - (1+v_1)\tau_1]T(b,t)}{\frac{a^2}{2a^2+2at+t^2}\left(\frac{v_1}{G_1} - \frac{1-2V_1}{G_2}\right) + \frac{1-2v_2}{2G_2} - \frac{1}{2G_1}} \tag{6}$$

Where τ_2 is coefficient of thermal expansion (CTE) of resin and τ_1 is that of ceramic, v_2 is Poisson ratio of resin and v_1 is that of ceramic, what's more, G_2 is shear modulus of resin and G_1 is that of ceramic

If the hoop stress δ_β is larger than the bending strength of ceramic shell σ_{slim}, then ceramic shell would crack, so the crack condition of ceramic shell could be represented as Eq. (7)

$$\delta_\beta \le \sigma_{slim} \tag{7}$$

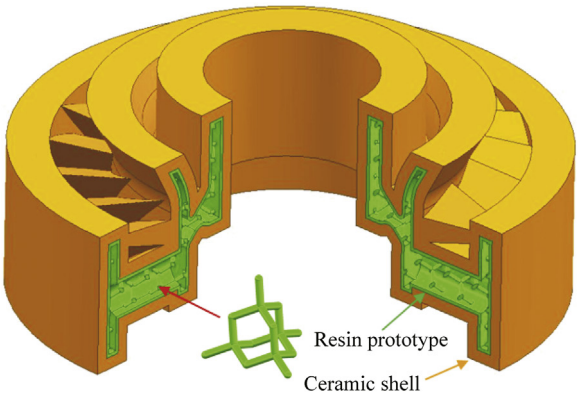

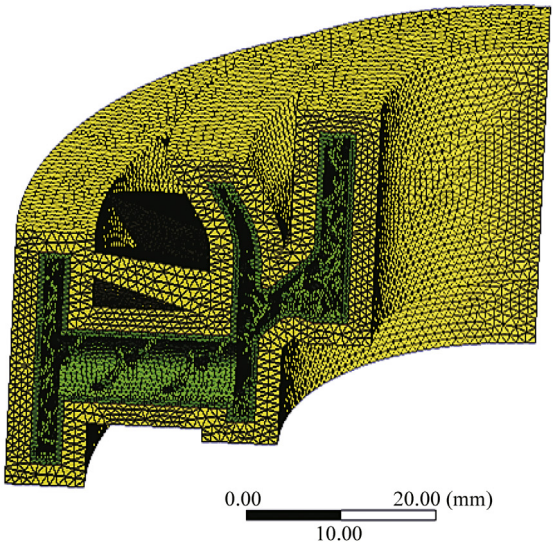

Figure 11 Analysis model and meshing model.

According to Eqs. (5)(6)(7) above, the hoop stress of ceramic shell can be reduced apparently so that shell cracking can be avoided by decreasing difference between resin's CTE and ceramic's CTE or decreasing wall thickness of resin prototype.

As the wall thickness of resin prototype with inner hollow structure is much lower than that of solid resin prototypes, what's more, the CTE difference between resin and ceramic is decreased when sintering the green ceramic shell under heating rate of 5 °C/min. Therefore, by sintering green ceramic shell with inner hollow resin prototype, the ceramic shell's thermal stress can be reduced and shell cracking can be avoided [9].

Table 2 Material properties.

Material	Elasticity modulus/MPa	Thermal conductivity/(W/(m · K))	Density/(kg/m^3)	Specific heat/(J/(kg · °C))	Poisson ratio	CTE/(10^{-6}/°C)
Resin	2399	0.132	1120	1050	0.23	see Figure 8
Ceramic	3200	19.5	5600	20	0.36	5

Table 3 Analysis scheme.

Number factor	1	2	3
Heating rate/(°C/min)	5	3	2

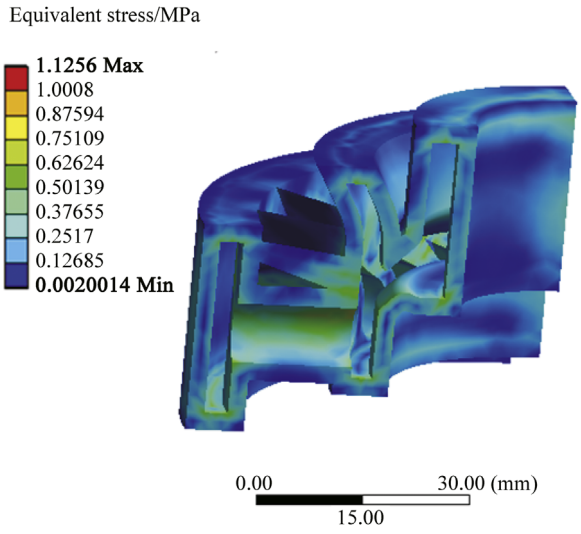

Figure 12 Thermal stress filed of ceramic shell under heating rate of 5 °C/min.

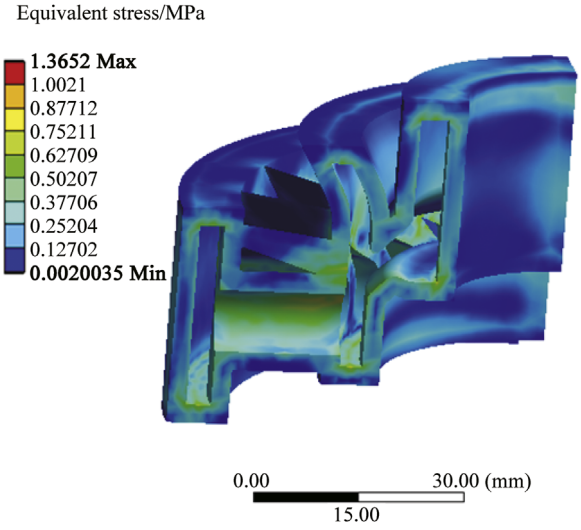

Figure 13 Thermal stress filed of ceramic shell under heating rate of 4 °C/min.

3.2.4. *FEA of thermal stress*

In fact, thermophysical properties of resin and ceramic change along with temperature rising. As the turbine structure of stator is more complex than that of cylinder, the thermal stress field of turbine stator cannot be completely explained by Eq. (7). Therefore, it is essential to investigate the law of ceramic shell's thermal stress field by using ANSYS software.

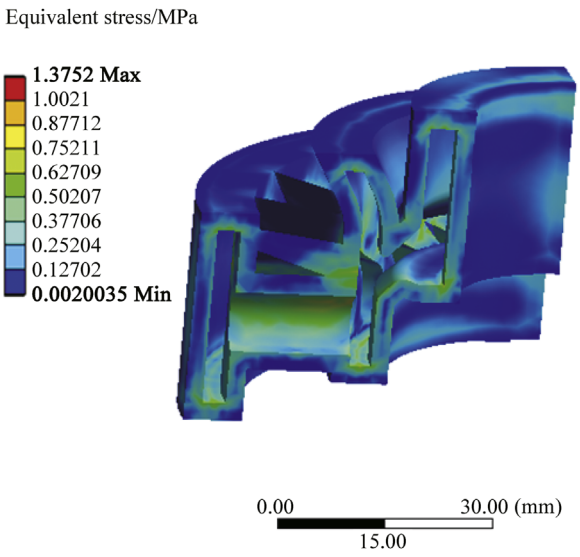

Figure 14 Thermal stress filed of ceramic shell under Heating rate of 3 °C/min.

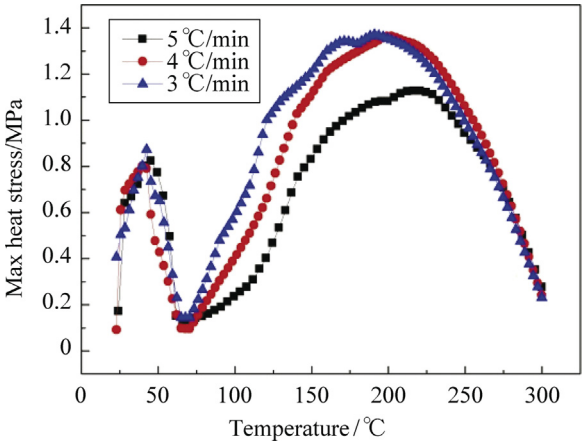

Figure 15 Comparison of maximum thermal stress.

3.2.4.1. Finite element model. The thermal stress fields under different temperature were calculated with the thermal-structure indirect coupling Equation of ANSYS software. Therefore, firstly the CAD model of resin prototype and ceramic shell were meshed (to reduce computing time, the whole CAD model is represented in one quarter as

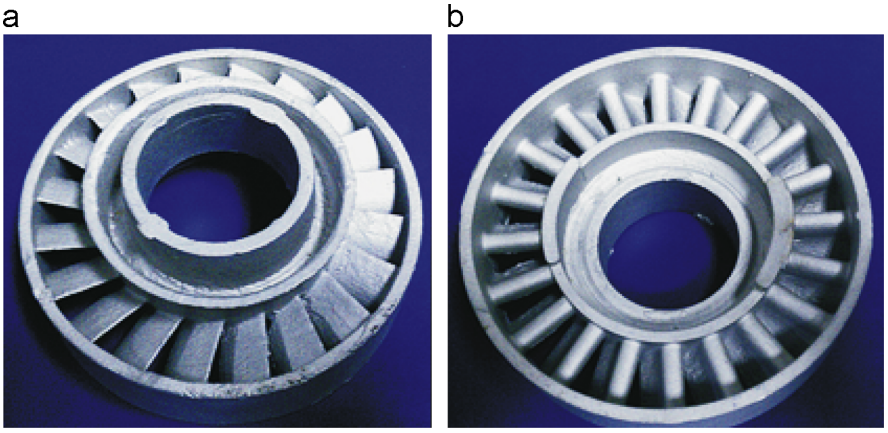

Figure 16 Metal turbine stator. (a) Upper face and (b) lower face.

is shown in Figure 11), then the material properties for CAD model are given in Table 2.

3.2.4.2. Result analysis. Thermal stress field of the ceramic shell was simulated from 20 °C to 300 °C. Because during the period, there is squeezing action between shell and resin caused by difference of thermal expansions, when the bending strength of ceramic shell is lower than maximum thermal stress, the ceramic shell would crack [9].

The thermal stress field under effect of resin prototype's inner hollow structure and different heating rates were investigated. And the analysis scheme is given in Table 3.

The thermal stress fields of ceramic shell under three different conditions are calculated by ANSYS software (Figures 12–14), the comparison of ceramic shell's maximum thermal stress under different heating rates is showed in Figure 15.

According to the Figure 15, there are two peaks of the thermal stress curves, at first, the curves increase to its first peak at about 48 °C, and then decrease until about 63 °C, after that the curves increase to the next peak at about 200 °C, which is the maximum thermal stress of ceramic shell, then the thermal stress decrease.

In addition, it is also clear that the heating rates effect on the thermal stress of ceramic is quite obvious. The maximum thermal stress decreases from 1.3714 MPa to 1.1272 MPa along with increment of the heating rate from 3 °C/min to 5 °C/min,

According to the results above, the maximum thermal stress of ceramic shell is 1.1272 MPa during pyrolyzing and sintering process when the ceramic shell with inner hollow resin prototype is sintered under heating rate of 5 °C/min. Therefore the maximum thermal stress of ceramic under that condition is lower than the bending strength of the ceramic shell (see Figure 6) and the shell cracking is avoided.

4. Experiment validations

Based on the analysis result above, the green ceramic shell was moved into a furnace under initial sintering temperature 20 °C, and then heated to 900 °C with heating rate of 300 °C/h and keep at 900 °C for 4 h. Finally the inside resin prototype was burned out entirely, a high accuracy and quality ceramic shell without shell cracking was obtained. The ceramic shell was heated to 600 °C, and then molten steel was poured into the ceramic shell under environment temperature of 1076 °C. The ceramic shell was cooled for 1 h after metal pouring, and then metal turbine stator (Figure 16) was acquired through shell cracking, sand blasting and surface polishing. The metal turbine stator's dimensional accuracy is CT4-CT6 and surface roughness R_a is within 3.2 μm.

5. Conclusions

This research combined stereolithography and investment casting to fabricate turbine stator, aiming at decreasing surface roughness of resin prototype and avoiding ceramic shell cracking. The surface roughness of resin prototype under effect of coating method was investigated using laser confocal microscopy; what's more, both theoretical analysis and FEA were combined and compared to reveal thermal stress field of ceramic shell during pyrolyzing and sintering process under different situation.

The staircases of resin prototype's surface were eliminated and the resin prototype's surface quality was improved apparently after it was treated by resin coating. Therefore surface staircases of resin prototype will not transfer to surface of the metal turbine stator after the QC process. The maximum thermal stress of ceramic shell was reduced by sintering ceramic shell with inner hollow resin prototype under heating rate of 5 °C/min, as the maximum thermal stress of ceramic shell was lower than maximum bending strength of the ceramic shell, so ceramic shell cracking can be avoided.

Finally, a coating process and a sintering process were proposed, then the intact SL-based ceramic shell for metal casting was achieved, the dimensional accuracy of metal turbine stator reached CT4-CT6 and the surface accuracy of it was within R_a 3.2.

Acknowledgements

This research works was supported by National Science and Technology Major Project (No. 2012ZX04007021). The authors are grateful for the grant.

References

[1] A.M. Evans, R.I. Campbell, A comparative evaluation of industrial design models produced using rapid prototyping and workshop-based fabrication techniques, Rapid Prototyping Journal 9 (5) (2003) 344–351.

[2] K. Dotchev, S. Soe, Rapid manufacturing of patterns for investment casting: improvement of quality and success rate, Rapid Prototyping Journal 12 (3) (2006) 156–164.

[3] D. Ahn, H. Kim, S. Lee, Surface roughness prediction using measured data and interpolation in layered manufacturing, Journal of Materials Processing Technology 209 (2) (2009) 664–671.

[4] D. Ahn, J.H. Kweon, S. Kwon, J. Song, S. Lee, Representation of surface roughness in fused deposition modeling, Journal of Materials Processing Technology 209 (15) (2009) 5593–5600.

[5] S. Wang, A.G. Miranda, C. Shih, A study of investment casting with plastic patterns, Materials and Manufacturing Processes 25 (12) (2010) 1482–1488.

[6] Y. Zhang, Y. Liu, J. Wang, Z. Han, Investigation on curing mechanism of phenylphenol modified phenol-formaldehyde resin by means of DSC method, Journal of Solid Rocket Technology 30 (2) (2007) 142.

[7] Y.Z. Tong, Improvement of surface finish by coating in stereolithography, Xi'an Jiaotong University, 2008, pp. 9–11.

[8] J. Chen, Y. Zhou, Elastic Mechanics, Shanghai, 2005, pp. 415–450.

[9] Y. Norouzi, S. Rahmati, Y. Hojjat, A novel lattice structure for SL investment casting patterns, Rapid Prototyping Journal 15 (4) (2009) 255–263.